The laser exposure requirements of liquid crystal polymer thin films for photomasking applications

David Goldie,*[a] James Cairns,[a] Mark Verrall[b] and David Coates[b]

[a]*Department of A.P.E.M.E., University of Dundee, Perth Road, Dundee, UK DD1 4HN*

[b]*Liquid Crystal Research, Merck Ltd, Quay Road, Poole, UK BH15 1TD*

Thin solid films of a cyanobiphenyl based polymethacrylate liquid crystal polymer (LCP) coated onto quartz substrates have been thermally processed to give a UV light scattering texture for use as a photomask opaque layer. UV transparent line patterns in the scattering layer may subsequently be written by scanning a focused laser beam across the LCP surface. The exposed linewidths are found to be strongly dependent upon the thickness of the LCP film, the incident power of the laser, and the overall residence time of the focused beam waist at a given location on the film surface. Successful exposure of the LCP films demands that the absorbed laser energy and beam waist residence time should exceed minimum threshold magnitudes however, and it is demonstrated that the smallest feature size which may be defined in the scattering layer is effectively limited by heat conduction from the LCP to the quartz substrate. Possible approaches towards improving the exposure requirements of the LCP are considered, and the compatibility of the proposed LCP photomask with current industrial direct-write laser systems is appraised.

The unprecedented growth in consumer products containing microelectronic components is largely founded upon the availability of cheap microchips which in many instances are designed to perform a particular self-dedicated function. Microchip manufacturers are constantly striving to increase the density of individual components on a single chip and to achieve this it is necessary that the smallest feature size which may be lithographically produced on a silicon wafer be continuously reduced. At present, feature sizes down to 0.3 μm may be routinely produced using standard ultraviolet (UV) photolithography which involves projection printing through a photomask onto silicon wafers coated with photoresist. The projection process normally uses optics to give an image reduction by a factor of 5 so that the smallest corresponding feature size recognisable on the photomask is about 1.5 μm.

Photomasks currently working down to a resolution of about 1 μm are conventionally produced using quartz plates coated with chromium. The chromium layer is typically 0.1 μm thick and is opaque at the standard UV wavelengths (designated G and I) used in projection lithography. The patterning of these photomasks to produce UV transparent tracks involves physical removal of the chromium however and this is a multistage process.[1] In particular, a detailed inspection of the photomask must always be made following the chromium etch process and time-consuming repairs performed to rectify identified defects in the chrome tracks. A schematic illustration of a chromium photomask is shown in Fig. 1(*a*). It should be noted that the finished product is often protected by a thin membrane layer (pellicle) before being shipped to the manufacturer. The pellicle prevents contamination of the photomask surface by dust particles and is an important consideration when it is realised that particulates lodged between the walls of the chromium tracks may be so strongly bonded as to be virtually immovable by high pressure water-jet cleaning.

The most costly processing stages incurred in the production of conventional photomasks (inspection, repair and pellicle application) fundamentally arise because patterning of the photomask requires physical removal of the UV opaque chromium. A preferred method of photomask fabrication would clearly involve direct writing of UV transparent regions onto the photomask opaque. Such a one-step approach would produce a photomask structure depicted in Fig. 1(*b*) where in this case, due to the retention of a continuous smooth surface on the photomask opaque layer, the provision of a pellicle is in principle no longer required. Potential materials for one-step photomask production are liquid crystal polymers (LCPs). The bulk optical properties of LCPs are sensitive to the relative order which exists between neighbouring domains and thus in the isotropic and non-isotropic phases of these materials the relative strength of optical scattering is accordingly classed as weak or strong respectively. Transformation between the strongly and weakly scattering phases may be reversibly accomplished through the application of an aligning electric field,[2] or by heating the material above a critical clearing-point temperature and quench cooling through the glass transition temperature of the polymer.[3] The electric field alignment properties have previously been proposed for the development of a photomask technology based upon liquid crystal cells[4] in which the LCP is maintained in a liquid state between plane-parallel aligning electrodes. By contrast, exploitation of the clearing point temperature phenomenon for photomask development involves depositing the LCP as a solid film onto a quartz substrate as depicted in Fig. 1(*b*). The LCP layer is then globally transformed into an optimised non-isotropic (strong-scattering) state by suitable thermal processing. Non-scattering regions in the LCP film may then be written by thermally inducing a local transition between the non-isotropic and isotropic phases. Previous work by the GEC group using polyacrylate LCPs has demonstrated that clear

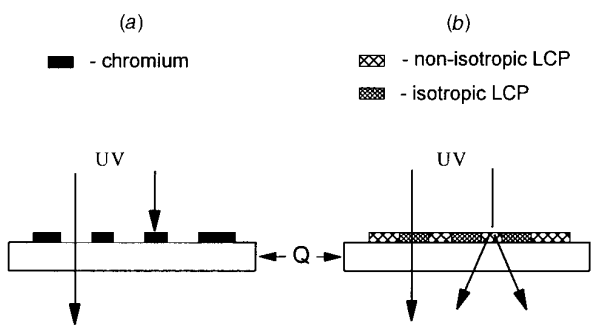

Fig. 1 Schematic illustration of the structure and operation of (*a*) a conventional chrome photomask and (*b*) an LCP photomask. Q = quartz substrate.

isotropic regions may be quenched into thin glassy films on flexible substrates by laser addressing at room temperature.[3,5] Negative contrast writing was produced on a non-isotropic scattering background with proposed applications for the polyacrylates as optical memory devices.

The present photomask work is also concerned with the production of clear regions on a scattering background by scanning the focused output from a laser across thin LCP films. A cyanobiphenyl based polymethacrylate LCP coated onto quartz substrates is used as the photomask opaque. The exposure requirements for the non-isotropic→isotropic writing process are experimentally determined, and the results used to evaluate whether LCPs provide a realistic commercial alternative to chromium for the fabrication of UV photomasks.

Experimental

Materials

The liquid crystal polymer identified as promising for initial investigation was a side chain cyanobiphenyl polymethacrylate coded LCP156 whose chemical structure is shown in Fig. 2. LCP156 possesses an average molecular mass $M_n = 38\,300$ and is characterised by a glass transition temperature T_g of 66 °C. In the non-isotropic liquid crystal phase, LCP156 has a high birefringence with the cyanobiphenyl side chains aligning in smectic A domains. The optically scattering liquid crystal phase becomes an isotropic liquid at a clearing point temperature T_c of 101 °C. By thermally processing LCP156 from temperatures above T_c to below T_g, the material becomes a glassy solid where the side chains are aligned in either the isotropic or non-isotropic states depending upon the rate of cooling through the liquid crystal phase. Slow cooling allows the pendant cyanobiphenyl groups to align in smectic A domains, whereas quench cooling freezes-in the isotropic liquid state.

The optical transmission spectrum of LCP156 reveals that the cut-off point for UV absorption in the polymer occurs at about 360 nm, with absorption becoming very strong below 350 nm. The material should therefore be compatible with UV photolithography at the G (436 nm) and I (365 nm) exposure wavelengths. To allow energy from the proposed HeNe laser writing wavelength of 633 nm to be efficiently coupled to LCP156, it was consequently necessary to add an anthroquinone based dye to the polymer. The spectral response of the anthroquinone dye (hereafter referred to as AQD) was measured at a 2.5% concentration in an isotropic host liquid and found to exhibit a maximum absorption at approximately 638 nm with an extinction coefficient of 44 l g cm^{-1}. The added concentration of AQD to LCP156 was nominally 2% by mass which maximised the laser absorption efficiency whilst ensuring that the dye did not crystallise out of the LCP.

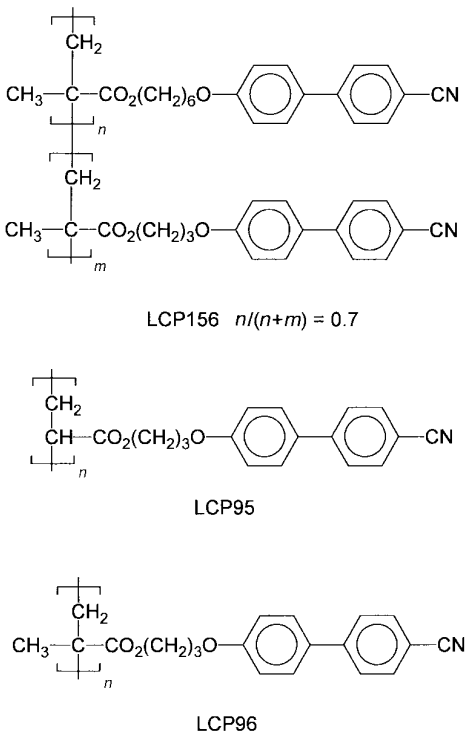

Fig. 2 Chemical structures of the LCPs used in the present work

Preparation of LCP solutions and spin-coating

Solutions of LCP156 suitable for spin-coating were prepared using cyclopentanone (C_5H_8O) as a solvent. Appropriate solution viscosities were obtained by adding accurately weighed amounts of the LCP156+AQD to measured volumes of C_5H_8O where the ratio of LCP156+AQD to solvent was varied between 5 and 60% by mass. In order to ensure complete dissolution of the polymer in the solvent, prepared solutions were generally allowed to stand for a period of 4–5 d in sealed glass vials. This solution formation period was particularly critical for more viscous concentrations where the mass ratio of polymer to solvent exceeded 30%. Immediately prior to spin-coating, the LCP solutions were routinely filtered using glass syringes fitted with 0.2 μm PTFE filters. This final filtering process was performed to remove contaminating AQD particulates which were observed to form in the C_5H_8O as a result of slow agglomeration of the dye molecules. As a result of filtering, the amount of AQD to LCP156 which remained in solution was somewhat reduced below the nominal 2% by mass concentration.

Thin films of LCP156+AQD were solvent cast from the above solutions using a standard spin-coating unit operating at speeds between 500 and 5000 rpm. Simple two-stage spinning programs involving a pre-spreading step followed by a coating step were found to produce uniform films on two-inch square quartz substrates. A surface profilometer (model Dektak^3 ST) was used to determine the thicknesses L_c of the dried LCP layers and to evaluate the associated surface roughness of the deposited films. For the range of C_5H_8O solution viscosities prepared, it was found that films having thickness varying between 0.5 and 10.5 μm could be reproducibly coated where the corresponding surface roughness of the layers was typically less than 2% of L_c.

Thermal processing of LCP films

The LCP films cast onto quartz substrates must be thermally processed in order to transform the layers into light scattering textures (*i.e.* to place the LCP into a non-isotropic state). The required thermal profile to achieve this is outlined in Table 1 and involves three basic stages; stage A: a heating step during which the specimen is raised above the clearing point temperature T_c; stage B: an annealing interval of duration t_{anneal} during which time the sample is held at a temperature $T_A > T_c$; stage C: a cooling period where the sample temperature is reduced to below the glass transition temperature T_g at a controlled cooling rate $(dT/dt)_c$.

To implement the above thermal recipe, an automated processing system was constructed which consisted of a custom-built hotplate linked to a HOTO TM55 temperature control unit. The hotplate was constructed using etched foil heaters to ensure a temperature accuracy of ±1 °C relative to the setpoint, and was fitted with under-plate nitrogen gas cooling at a working pressure of 30 psi to permit cooling rates approaching 5 K min^{-1} to be readily achieved. The controller unit was equipped with a serial interface to allow remote

Table 1 Thermal processing procdure used to transform LCP films into a non-isotropic state. T_A annealing temperture; T_g glass transition temperature

stage	thermal process	temperature range	t/min
A	heat to T_A	room temp.$\rightarrow T_A$	20
B	anneal	T_A	t_{anneal}
C	cool through T_g	$T_A \rightarrow (T_g-20)$	$[T_A-T_g+20]/(dT/dt)_c$

control *via* a computer, and software was developed to handle stages A–C in Table 1.

To determine the optimum cooling rate required to induce maximum scattering for LCP156, a number of identically prepared films were thermally processed into an optical scattering state keeping T_A ($=130\,^{\circ}C$) and t_{anneal} ($=15$ min) constant, but using different values for $(dT/dt)_c$. Optical transmission experiments conducted on these samples revealed that the scattering power of LCP156 is relatively insensitive to the cooling rate but appears to be maximised in the vicinity of $(dT/dt)_c = -1$ K min^{-1}. This was therefore adopted as the standard cooling rate for thermal processing of LCP156 into an optimised non-isotropic state.

The integrity of the LCP layers following thermal processing was evaluated by comparing the surface profiles of films in the isotropic and non-isotropic phases. For a single thermal process stage, the surface roughness of the layers was observed to remain essentially unchanged from the as-cast magnitude, though repeated thermal cycling was found to progressively increase the surface roughness by a factor of *ca.* 3 after the completion of 8–10 cycles. Thermal processing of the films into the non-isotropic phase was additionally found to reduce the average film thickness to about 90–95% of L_c. Shrinkage of the films was only noticeable following the first thermal process cycle however and is therefore believed to be associated with a reduction in free volume of the LCP following internal reorientation of the polymer matrix at elevated temperatures. Overall, the changes observed for both the thickness and surface roughness of the processed films are relatively small, and these phenomena are not considered to represent a major drawback to the use of LCP156 as a photomask opaque material.

Laser writing on LCP films

The laser selected to perform writing tests on the LCP photomasks was a commercially available HeNe unit operating in a continuous wave mode at 633 nm with a nominal power output of 13 mW. The quoted output beam parameters were a beam waist of 800 μm, a beam divergence of 1 mrad and a Rayleigh distance of 80 cm. In order to successfully write clear isotropic regions on the photomask, the amount of energy absorbed from the beam must be sufficient to locally raise the temperature of the LCP above T_c. To achieve this a singlet lens having a focal distance of 0.7 cm was used to reduce the beam waist to 6 μm. By modifying the output beam with the focusing lens, the transformed beam divergence was estimated from simple gaussian optics to increase to 133 mrad and the corresponding focal depth to be reduced to 45 μm.[6] The laser and auxiliary deflecting mirrors were consequently mounted along the (x-) axis of an optical guide, with the samples to be irradiated being attached in a horizontal plane to the arm of an x–y chart recorder under the focusing lens. The chart recorder was fitted with a manual y-adjustable platform, and modulation of the x-input of the unit with a ramp drive allowed the photomasks to be scanned beneath the singlet lens at accurately controlled speeds v_s between 0.01 and 3 cm s^{-1}. Due to the relatively small depth of focus, the singlet lens holder was connected to a micro-positioner arm to provide sensitive control over the lens to film distance in the z-direction.

In addition to continuous scanning of the focused beam across the LCP surface, a number of experiments were conducted in which the photomask was held stationary and exposed to the incident beam for a finite time t_p. A mechanical shutter was used to chop the continuous output from the laser and in this manner light pulses down to $t_p \sim 0.2$ ms were produced. It is straightforward to show that under pulsed conditions, the exposed area of LCP film receives an amount of energy from the incident beam which would be obtained by continuous scanning at a speed given by eqn. (1)

$$v_s = d_o/t_p \quad (1)$$

where d_o is the diameter of the focused beam waist. For $d_o =$ 6 μm, the effective scan speed which can be experimentally realised is therefore extended to 30 cm s^{-1} by pulsed exposure.

Results and Discussion

Measurement of written linewidths

Visual inspection of isotropic features written onto the LCP photomask was conducted using a microscope equipped with a CCD camera and a calibrated on-screen video measurement unit which allowed linewidths ($2r_l$) and spot diameters ($2r_d$) to be directly measured. Examples of lines written onto a 5.4 μm LCP156 film are shown for scanning speeds of 1.2 cm s^{-1} in Fig. 3(*a*), and 3.0 cm s^{-1} in Fig. 3(*b*). Small dots written onto the same film under pulsed conditions are also shown where the exposure times have been selected to give the same effective scan speeds according to eqn. (1). It is

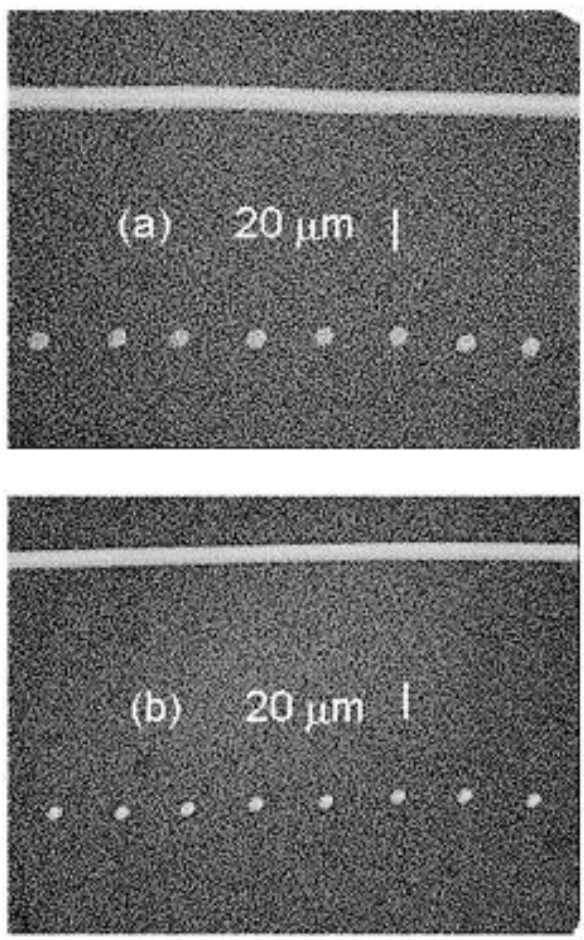

Fig. 3 Examples of isotropic features written onto a 5.4 μm thick LCP156 photomask using a 13 mW HeNe laser: (*a*) line scan speed $v_s = 1.2$ cm s^{-1}, pulsed exposure time $t_p = 0.5$ ms; (*b*) line scan speed $v_s = 3.0$ cm s^{-1}, pulsed exposure time $t_p = 0.2$ ms

evident that for equivalent exposure times the measured spot diameters closely agree with the corresponding linewidths (*i.e.* $2r_d = 2r_l$). The majority of work conducted on determining the dependence of written isotropic feature dimensions upon laser exposure conditions was consequently carried out using pulsed excitation due to the greater range of scan speeds accessible, and the potential to statistically determine average values for $2r_d$ from the measured diameters of a large number (*ca.* 20) of identically written dots.

Dependence of $2r_d$ on exposure conditions

Effect of varying the LCP film thickness. A series of spot writing experiments were conducted on samples of LCP156 + AQD in which the as-cast film thickness L_c was varied between 1.65 and 10.0 μm. The incident laser power was held fixed at 13 mW in all cases and exposure times t_p ranged from 0.2 to 20 ms. The results of these tests are summarised in Fig. 4 where the measured spot diameters $2r_d$ are plotted as a function of L_c. The following features of the data are noted: (*i*) As L_c increases $2r_d$ displays a tendency to saturate. (*ii*) Below a minimum threshold thickness it is impossible to write on the films.

Both of the above observations may be interpreted with reference to the amount of energy absorbed from the HeNe beam. For sufficiently large L_c, the amount of absorbed energy is maximised and depends upon the amount and optical response of the incorporated dye. For AQD at an added mass concentration approaching 2%, it is estimated that about 98% of the incident light is absorbed when $L_c = 10$ μm, and the saturated spot size is dictated by the maximum temperature rise locally induced by the corresponding absorbed energy. Conversely, when L_c falls below some critical limit L_c^* the amount of absorbed energy is insufficient to cause the local temperature rise to exceed T_c and the LCP remains in a non-isotropic scattering state. It should be noted that, irrespective of how long one makes t_p, no spot features may be written when $L_c < L_c^*$. This phenomenon is simply a manifestation of the fact that for sufficiently long times, the temperature at any location within the film attains a local maximum value representative of some global equilibrium state. The equilibrium is dynamic in nature such that the rate of energy input P_{abs} is exactly balanced by a rate of energy loss for any selected volume element within the LCP film. Consequently, to ensure that the temperature exceeds T_c at some point within the film, P_{abs} must exceed a threshold magnitude P_{abs}^*, and since (for a fixed incident HeNe power) $P_{abs} \propto L_c$ we require that $L_c > L_c^*$. To estimate the critical thickness L_c^* from Fig. 4, regression curves shown as solid curves were fitted to the data points for the various exposure times used. The simplest form of analytical expression found to provide an acceptable regression fit was logarithmic in nature such that eqn. (2) holds.

$$(2r_d) = a + b \times \log_e(L_c) \quad (2)$$

The required values of the adjustable fitting parameters a and b were 7.2 and 11.9 μm, respectively. Whilst it is appreciated that such an expression can only provide an empirical fit to the data and has no physical basis [$2r_d$ does not saturate with L_c according to eqn. (2)] it may usefully be employed in the low L_c region to determine L_c^*. Thus, setting $2r_d = 0$ in eqn. (2), the extrapolated value of L_c^* using the a and b fitting parameters is found to be 0.55 ± 0.17 μm. For this threshold thickness, the fraction of incident light absorbed is only 20% and P_{abs}^* is correspondingly calculated to be 2.60 ± 0.65 mW.

Effect of varying the incident HeNe irradiation power. An independent check of the P_{abs}^* magnitude was made by directly measuring the threshold HeNe power required to write an isotropic spot feature. Variation of the incident HeNe power between 0.5 and 13 mW was achieved by attenuating the output beam through the use of neutral density filters. Pulsed writing tests with $0.2 < t_p < 5$ ms were performed on LCP156 films 9.4 μm thick for which the amount of absorbed light energy was estimated to be 98%. A typical set of results is shown in Fig. 5 which displays the measured spot diameters $2r_d$ as a function of the incident HeNe power. The important observations to be noted from these data are as follows. (*i*) For a chosen t_p, the spot diameters become larger as the incident power is increased. This presumably reflects the greater increase in maximum local temperature induced for higher incident powers and parallels the increase in spot diameter found with increasing L_c in Fig. 4. (*ii*) The rate of increase of $2r_d$ with incident power is dependent upon t_p, with a faster increase accompanying longer exposure times. Once again this is connected with the comparative maximum temperature rises expected locally. (*iii*) Below a minimum threshold power of 2.6↔3.9 mW, it is impossible to write spot features onto the films irrespective of the length of illumination time t_p. This corresponds to the fact that at these powers, $P_{abs} > P_{abs}^*$ is not being fulfilled.

From (*iii*) above, the threshold power is therefore directly measured to lie between 2.6 and 3.9 mW taking into account the small correction factor of 0.98 due to incomplete absorption. P_{abs}^* is accordingly estimated as $P_{abs}^* = [(2.6 + 3.9)/2] \times 0.98 = 3.20 \pm 0.65$ mW. This value is to be compared with the figure of 2.60 ± 0.65 mW deduced from Fig. 4.

Dependence of written spot size on illumination time t_p. In order to successfully write onto LCP156 photomasks it is necessary to ensure that not only does the absorbed power exceed P_{abs}^*, but also that the exposure time t_p is sufficiently

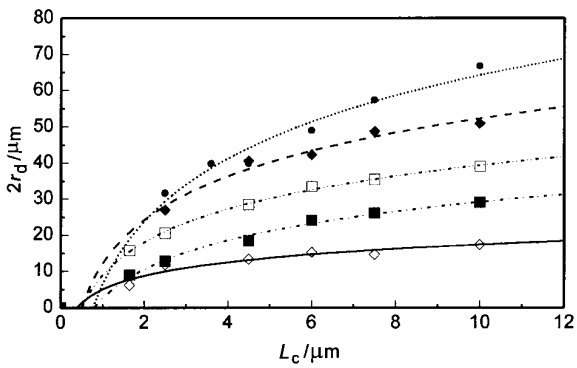

Fig. 4 Dependence of measured spot diameters $2r_d$ upon film thickness L_c for LCP156 + AQD films. The incident laser power was 13 mW and the exposure times t_p were respectively (◇) 0.2, (■) 1.0, (□) 5.0 and (◆) 20.0 ms. The saturated data (●) corresponded to $t_p = 10$ s.

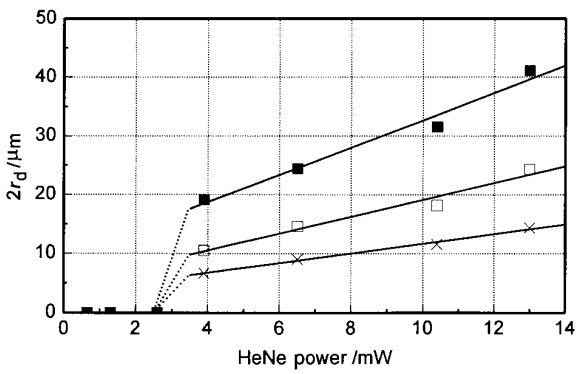

Fig. 5 Dependence of measured spot diameters $2r_d$ upon incident laser power for LCP156 + AQD films. The film thickness was 9.4 μm and the exposure times t_p were (■) 5.0, (□) 1.0 and (×) 0.2 ms.

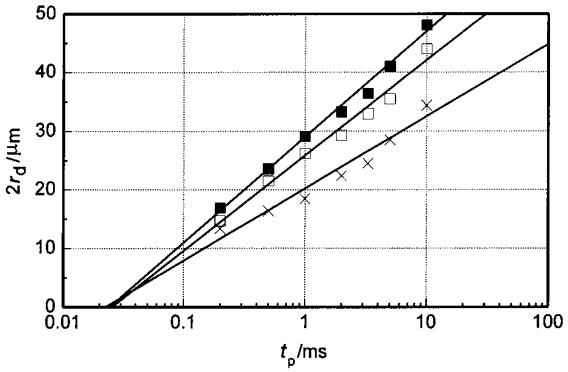

Fig. 6 Dependence of measured spot diameters $2r_d$ upon illumination time t_p for LCP156+AQD films. The film thicknesses were (■) 9.4, (□) 7.5 and (×) 4.5 μm.

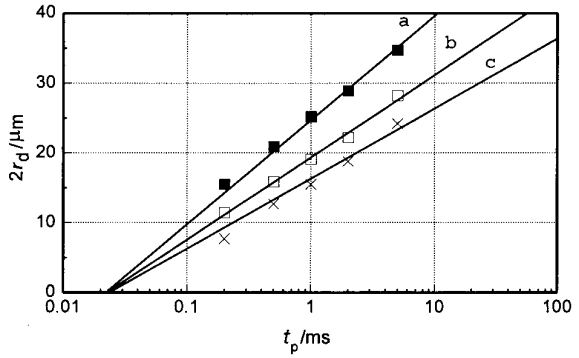

Fig. 7 Dependence of measured spot diameters $2r_d$ upon illumination time t_p for a 10.0 μm thick LCP156+AQD film. The incident HeNe powers were (■) 13.0, (□) 10.4 and (×) 6.5 mW.

longer than some as yet undetermined onset time t_p*. The requirement that $t_p \geqslant t_p$* is obvious from the data already presented in Fig. 4 and Fig. 5 where spot diameters $2r_d$ become progressively smaller as the exposure time is reduced. The question which arises is what is the functional dependence of $2r_d$ upon t_p and does this imply that written spot features will vanish before t_p is reduced to zero?

Data illustrating an apparent logarithmic variation of $2r_d$ with t_p are presented in Fig. 6. These results were obtained on films of LCP156 having different thicknesses which were subjected to an incident HeNe power of 13 mW. The fitted regression curves assume the form eqn. (3),

$$(2r_d) = a + b \times \log_e (t_p) \quad (3)$$

where a and b are fitting parameters. It was found that eqn. (3) provided an excellent fit to the data in the time regime where $t_p \leqslant 10$ ms and the regression parameters are summarised in Table 2.

For longer t_p, the spot diameters display a tendency to saturate and eqn. (3) is not applicable. This is confirmed by the columns in Table 2 comparing measured diameters at $t_p =$ 10 s with extrapolated values from the fitted curves. It is recognised that the functional format of eqn. (3) has no physical foundation and is purely empirical. The following points are noted from Fig. 6. (*i*) The rate of increase of $2r_d$ with t_p is dependent upon the film thickness L_c. This of course simply reflects the fact that P_{abs} is greater for thicker films. (*ii*) Extrapolation of the regression curves to $2r_d = 0$ suggests that $t_p^* \sim 0.025$ ms. The onset time appears to be independent of L_c and hence P_{abs}.

To verify that t_p* is indeed independent of P_{abs}, a second set of exposure time experiments were conducted on a 10.0 μm film in which the incident HeNe power was attenuated directly. Results obtained for 13, 10.4 and 6.5 mW are shown in Fig. 7 and once again extrapolate in all cases to $t_p^* \sim 0.025$ ms.

The apparent independence of the threshold exposure time t_p* upon P_{abs} is interesting as it implies that the use of progressively higher incident powers will not permit successful exposure to occur for correspondingly shorter times. Such a limitation may be connected with the flow of heat within the LCP film and the failure to attain local temperatures greater than T_c. Alternatively, t_p* may represent the minimum time required for key molecular relaxation processes to occur in the transformation between the non-isotropic and isotropic phases of the LCP.

Table 2 Summary of regression parameters used to fit the data of Fig. 6 using eqn. (3). t_p* is the extrapolated onset exposure time below which spot features cannot be written. (*i*) Extrapolated spot diameter at $t_p = 10$ s from regression parameters; (*ii*) measured spot diameter at $t_p = 10$ s

L_c/μm	a	b	t_p*/ms	$2r_d^{(i)}$/μm	$2r_d^{(ii)}$/μm
4.5	20.2	5.3	0.023	69.0	39.9 ± 1.6
7.5	25.8	7.1	0.026	91.2	57.4 ± 1.7
9.4	29.0	7.8	0.025	100.8	66.8 ± 5.9

Estimation of the exposure requirement of LCP156+AQD under HeNe illumination

From the data analysed above we are now in a position to estimate the minimum exposure requirements of LCP156. We have seen that the threshold input power is $P_{abs}^* \approx 2.9$ mW, and that this rate of energy input must be maintained for a minimum exposure period of $t_p^* = 0.025$ ms. The resulting energy threshold E^* is accordingly given by eqn. (4),

$$E^* = P_{abs}^* \times t_p^* \quad (4)$$

so that $E^* = 2.9\ \text{mW} \times 2.5 \times 10^{-5}\ \text{s} = 73$ nJ. This energy is effectively delivered over an area of the film surface bounded within the focused HeNe beam waist. Since the calculated beam waist is 6 μm, the corresponding exposure area is 28.3 μm^2 and the exposure sensitivity of LCP156 is therefore 73 nJ/28.3 μm^2 = 258 mJ cm^{-2}. This estimate is consistent with the typical order of magnitude figure of >100 mJ cm^2 quoted for this class of LCP material.[2]

Approaches towards reducing the exposure requirements of LCP photomasks

The exposure sensitivity of LCP156 calculated above is in practice an upper limit since it has been implicitly assumed that all of the absorbed optical energy is converted into heat within the LCP alone. This situation is clearly unrealistic as heat loss to the surroundings is anticipated to be significant. Potential energy sinks include radiative and convective processes at the LCP surface, but the most important channel for heat dissipation from the LCP layer is suspected to involve direct heat conduction into the substrate. Possible approaches to improve the exposure sensitivity of the LCP photomasks are now discussed.

Substrate selection. An obvious approach to reduce heat flow into the substrate is to employ a substrate material possessing a relatively poor thermal conductance. The quartz substrates presently employed have a thermal conductance K_v of approximately 10^{-3} W cm^{-1} K^{-1}.[7] In order to achieve a noticeable improvement in thermal insulation between the LCP and substrate, it is predicted from thermal simulation data[8] that the thermal conductivity of the substrate [K_v(sub)] will need to be an order of magnitude lower than the thermal conductivity of the LCP which is estimated as K_v(LCP156) ~ 10^{-3} W cm^{-1} K^{-1}.[2] However, a survey of

potential substrate glasses reveals that few possess K_v values significantly smaller than quartz. Irrespective of whether a suitable low K_v glass does exist, the substrate material must primarily possess the necessary optical properties to function in a photomask environment.† For this latter reason, it is difficult to envisage that the microelectronics industry would consider replacing quartz as the photomask substrate and an alternative approach towards improving the exposure sensitivity of the LCP photomasks must be proposed.

Thermal buffering between the LCP layer and substrate. A possible solution to reduce conductive heat loss from the LCP is to insert a thermally insulating buffer layer of thickness L_b between the LCP layer and substrate. The buffer material selected must be optically inert at the standard G and I UV wavelengths employed in projection printing and for this reason should be kept as thin as possible (for example $L_b \leqslant 2$ μm which would represent some 20–25% of a typical LCP thickness). The requirement that the buffer layer remains thin places a greater demand on the efficiency of thermal insulation provided by the selected material and simulation studies suggest that for $L_b \leqslant 2$ μm, $K_v(\text{lcp})/K_v(\text{buffer})$ should be greater than 10 in order to be effective.[8]

Initial experimental work using thermal buffers has focused upon an isotropic polymer (coded LCP96) whose chemical structure is illustrated in Fig. 2. This material has a molecular mass of 23 000 and a glass transition temperature of 84 °C. The thermal conductivity of LCP96 is believed to be comparable to that of LCP156.[2] Films of LCP96 ranging between 0.8 and 2.0 μm were deposited onto quartz substrates by spin-coating from cyclopentanone solutions. Following a suitable drying period, the buffer layers were then thermally processed using standard conditions to remove residual solvent and allow for possible film shrinkage. Identical layers of LCP156 + AQD 10.4 μm thick were finally spin-coated onto these pre-coated substrates, with the entire structures being thermally processed for a second time to place the LCP156 into a scattering state.

The results of pulsed experiments using different LCP96 thicknesses are compared in Fig. 8. The incorporation of the LCP96 layer is found to have a negligible effect upon the measured spot diameters. Effective thermal buffering between LCP156 and the substrate would have resulted in enhanced lateral heat flow and larger values of $2r_d$ for a given exposure time t_d. The thermal conductivity of LCP96 is consequently too high to provide effective insulation for $L_b \leqslant 2$ μm.

Reduction of LCP transition temperature through chemical modification. The most direct approach towards reducing the LCP exposure requirements is to reduce the clearing point transition temperature T_c. This may be accomplished through chemical modification of the underlying polymer structure. In order to function reliably in a photomask projection environment however, T_c is effectively constrained to exceed a minimum value for the following reasons. (*i*) T_g should always be higher than the maximum operating temperature of the LCP photomask which under projection printing conditions may reach $T_{proj} \sim 40$ °C. In order to form a scattering texture and maintain image integrity, T_c must exceed T_g by a margin of about 30 °C however so that a practical minimum limit for T_c is about 70 °C. (*ii*) Reducing the clearing point temperature of the LCP is often accompanied by a decrease of the associated glass transition temperature T_g. To ensure that the mechanical properties of the LCP film remain robust, T_g should at least exceed T_{proj} so that T_g (minimum) ~ 40 °C.

With the above criteria in mind, a new LCP (coded LCP95 and shown in Fig. 2) having $T_c = 85$, $T_g = 49$ °C and $M_n = 5900$ was evaluated as a photomask opaque. The clearing temperature of LCP95 is 16 °C lower than that of LCP156 and should consequently show an enhanced response (*i.e.* larger spot diameters) under comparable exposure conditions (*i.e.* incident laser powers and exposure times). Data apparently consistent with these predictions are shown in Fig. 9 where a direct comparison is made between spot diameters for 3.3 μm thick films of LCP95 and LCP156. Significantly, it is noted from the extrapolated regression curves that the threshold exposure time t_p* is reduced by almost a factor of 2 for LCP95. The minimum incident power P_{abs}* to write onto LCP95 films was estimated to lie between 1.9 and 2.9 mW so that the overall exposure E* for the new polymer is calculated to be $E^* \sim 33 \pm 7$ nJ. The corresponding sensitivity of LCP95 is therefore 117 ± 25 mJ cm^{-2} which is a factor of 2–3 lower than LCP156. Reduction of the clearing point transition temperature by comparatively modest amounts would thus appear to result in significant improvements in LCP sensitivity.

Response of LCP materials to industrial laser writing systems

It is important to establish whether the current LCP materials will respond positively to the writing conditions prevalent in direct-write-lasers (DWLs) commonly employed by industrial mask makers. With the results presented above, we are now in a position to predict whether exposure of the LCP photomask will be successful, based upon the nominal specification of the laser writing equipment. The DWL systems of primary importance within the mask-making industry are the Core 2564 system marketed by ETEC INC., and the HeCd and Argon DWLs marketed by Heidelberg Instruments. The principal operating characteristics for each of these systems is summarised in Table 3 where information has been drawn

† Quartz displays virtually no absorption at the UV wavelengths currently employed in projection printing.

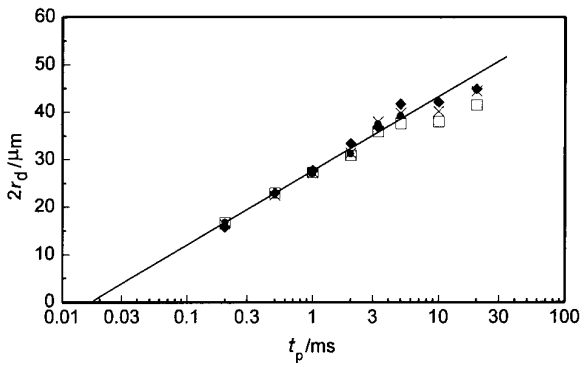

Fig. 8 Comparison of measured spot diameters $2r_d$ for 10.4 μm thick LCP156 + AQD films deposited onto a thermal buffer layer (LCP96). The thickness of the buffer layers were (□) 0, (●) 0.8, (×) 1.1 and (◆) 2.0 μm.

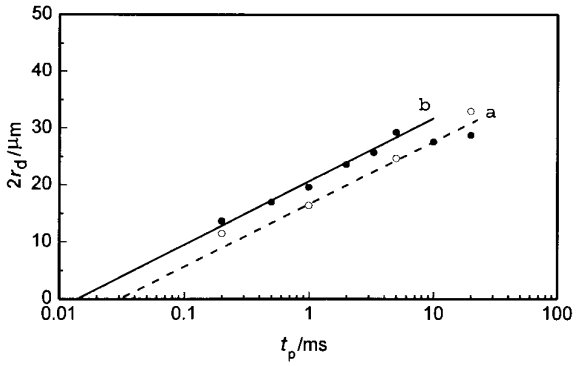

Fig. 9 Comparison of measured spot diameters $2r_d$ for polymers LCP156 and LCP95 containing nominally equal amounts of AQD: (○) LCP156 and (●) LCP95. The film thickness was 3.3 μm in both cases.

Table 3 Operating conditions for some industrial DWLs. The laser used in the present work (HeNe) is included for reference

DWL system	wavelength /nm	power /mW	beam waist /μm	$4P/\pi d_o^2$	scan speed /cm s^{-1}	exposure time t/s	energy density E /mJ cm^{-2}
HeNe	633	13	6.0	5e7	<30	$>1\times10^{-4}$	5520
Core 2564	364	3	1.0	4e8	1250	8×10^{-8}	30
Heidelberg HeCd	442	10–20	0.8	3e9	4000	2×10^{-8}	40–80
Heidelberg Ar	514	1000	0.8	2e11	4000	2×10^{-8}	4000

primarily from the respective supplier's documentation.[9] The exposure conditions employed for the current HeNe setup have also been included for reference.

For LCP156 it has been established that for successful film exposure to occur the following three conditions must be simultaneously fulfilled. (*i*) The absorbed energy density E must exceed the critical threshold E^* for the photomask material. For LCP156, the sensitivity E^* was determined to be 258 mJ cm^{-2}. (*ii*) In addition to (*i*), $4P/\pi d_o^2$ for the selected addressing laser must exceed $4P_{abs}^*/\pi d_o^2$ where P_{abs}^* is the critical threshold power absorbed by the film for a focused spot diameter d_o. For LCP156 $P_{abs}^* \approx 3.2$ mW and so $4P/\pi d_o^2$ must exceed 1.1×10^7 mW cm^{-2}. (*iii*) In addition to (*i*) and (*ii*), the exposure time for the selected addressing laser must exceed t_p^* where t_p^* is the critical minimum exposure time. For the present HeNe setup, it has been established that $t_p^* = 2.5\times10^{-5}$ s for LCP156.

Assuming that appropriate dyes may be selected to ensure almost 100% energy-coupling at the various laser wavelengths, a survey of the system specifications collected in Table 3 reveals the following. The Core and Heidelberg HeCd systems would fail to provide LCP156 with sufficient energy E to induce an exposure. The absorbed power density in both cases fulfil criterion (*ii*) however and the difficulty lies with too short an exposure period t_p such that (*iii*) is not satisfied. Both of these systems require the scanning rate to be reduced by a factor of 300–1000 in order to expose LCP156 photomasks. The Heidelberg Ar system satisfies conditions (*i*) and (*ii*) but t_p is still a factor of about 1000 too short to allow successful exposure of LCP156. A considerable reduction in scanning speed is therefore also required if this system is to to provide a positive response.

Conclusions

The main points arising from the present work may be summarised as follows.

(*i*) Pulsed experiments conducted using a HeNe laser have allowed the exposure sensitivity E^* of LCP156+AQD films to be estimated. For layers coated onto quartz substrates, $E^* \sim 258$ mJ cm^{-2}. This figure represents an upper limit to the underlying sensitivity of the LCP as no corrections have been made for heat loss to the substrate or surrounding air.

(*ii*) Attempts to reduce E^* by incorporating a thermal buffer layer (LCP96) between the LCP and substrate have proved unsuccessful. The failure of LCP96 has been attributed to its comparatively high thermal conductivity. For thermal buffering to be effective using relatively thin (<2 μm) layers it is predicted that the insulating material should posses a thermal conductivity of less than a tenth of the overlying LCP.

(*iii*) The exposure sensitivity may be improved by chemically modifying the LCP to reduce the clearing point temperature T_c. Pulsed exposure experiments performed upon LCP95 for which $T_c \sim 85$ °C indicate that $E^* \sim 117$ mJ cm^{-2}.

(*iv*) It has been established that in addition to the requirement that the sensitivity threshold E^* be exceeded, successful exposure of LCP156 films will only occur if the absorbed laser power and exposure times are greater than critical magnitudes P_{abs}^* and t_p^* respectively. For LCP156 films on quartz substrates, $P_{abs}^* \sim 1.1\times10^7$ mW cm^{-2} and $t_p^* \sim 2.5\times10^{-5}$ s. P_{abs}^* is believed to be governed by heat loss from the LCP and should therefore be reduced by thermal buffering. The physical origin of t_p^* is less certain but may also be connected with the dynamics of heat flow; alternatively, t_p^* may be indicative of a fundamental minimum time required to perform molecular reorientation between the isotropic and non-isotropic states. It has been shown experimentally that t_p^* is reduced as T_c is lowered.

(*v*) Currently available industrial DWLs are incapable of exposing LCP156 photomasks. For all industrial systems, unsuccessful exposure is a direct consequence of the scanning speeds being too high and the effective exposure times being correspondingly too short.

References

1 S. P. Murarka and M. C. Peckerar, in *Electronic Materials—Science and Technology*, Academic Press Inc., London, 1989.
2 *Side Chain Liquid Crystal Polymers*, ed. C. B. McArdle, Blackie, Glasgow and London, 1989.
3 C. Bowry and P. Bonnett, *Optical Computing and Processing*, 1991, **1**, 13.
4 Patent references (date of filing): (*a*) WO,A,90 10047 (1990); (*b*) GB,A,2 188 748 (1986); (*c*) GB,A,2 217 862 (1989); (*d*) US,A,4 013 466 (1975).
5 C. Bowry, P. Bonnet and M. Clark, *Proceedings Eurodisplay 90*, Amsterdam, p. 158.
6 D. O'Shea, *Elements of Modern Optical Design*, John Wiley and Sons Ltd., Chichester, 1985.
7 *Handbook of Chemistry and Physics*, CRC, 49th edn., section E-8.
8 D. M. Goldie, simulation data, 1995 (unpublished).
9 (*a*) DWL technical specification, Heidelberg Instruments, Mikrotechnik, Tullastrasse 2, 69126, Heidelberg; (*b*) Core 2564 Technical Overview, ETEC Systems Inc., 9100 SW Gemini Drive, Beaverton, OR 970015, 1993.

Paper 7/02841E; *Received* 25*th April*, 1997